Chapter 3
Vibration Measurement and Mitigation Development for Multi-Shaker Test Stand

Maura C. Hart, Jackson A. Jones, Kyle Crapo, Madyson G. Hodson, Connor Crandall, Mason Rollans, Matthew S. Allen, and Michael Denison

Abstract Multiple Input Multiple Output (MIMO) vibration testing is used in many industries to simulate the environmental conditions that components will encounter, allowing for the assessment of their durability. A modular frame mounted with multiple shakers has been developed by Sandia National Laboratories that can produce complex vibration environments at a fraction of the cost and setup time currently required by typical shaker systems. MIMO random vibration testing aims to replicate the complex vibrations of a Device Under Test (DUT) by precisely controlling the drive signal sent to each shaker. In some test conditions, this setup experiences a sharp rise in drive voltage, which can make the test impossible to run with available shakers or amplifiers. The vibration environment within the frame itself has not been studied, and may be the source of these test failures. To better understand the dynamics of the test frame, a roving hammer modal test was conducted to identify the vibratory modes of the frame within the frequency band normally used for random vibration testing (20-2000 Hz). A single-shaker configuration was used to excite a suspended test article and the frame's response was measured. Two vibration treatments—viscoelastic isolation and particle damping—were explored. Their damping effect on antiresonance amplitude and drive voltage to the test article was quantified. It was found that the particle damping method was consistently effective at damping all frequencies, while viscoelastic damping had varied results depending on frequency and configuration. In the system studied here, the particle damping treatment decreased the RMS shaker voltage by a factor of 2 across the full test range and up to a factor of 20 around the antiresonances.

Keywords Dynamic testing environment · NEWT · Passive damping · Particle damping · Viscoelastic isolator

Introduction

Dynamic environment testing is essential for the structural qualification testing of everything from aerospace components [1] to consumer products [2]. Tests in industry are dominated by single-axis tests on large shakers, yet there is increasing

Maura C. Hart · Jackson A. Jones · Kyle Crapo · Madyson G. Hodson · Connor Crandall · Mason Rollans
Undergraduate Students, Brigham Young University, Department of Mechanical Engineering
e-mail: hartmc11@byu.edu; jaj268@byu.edu; kcrapo3@byu.edu; mgd35@byu.edu; ccran29@byu.edu; mrollans@byu.edu

Matthew S. Allen
Professor, Brigham Young University, Department of Mechanical Engineering, matt.allen@byu.edu
e-mail: matt.allen@byu.edu

Michael Denison*
Senior Members of Technical Staff, Sandia National Laboratories
e-mail: mdeniso@sandia.gov

*This article has been authored by an employee of National Technology & Engineering Solutions of Sandia, LLC under Contract No. DE-NA0003525 with the U.S. Department of Energy (DOE). The employee owns all right, title and interest in and to the article and is solely responsible for its contents. The United States Government retains and the publisher, by accepting the article for publication, acknowledges that the United States Government retains a non-exclusive, paid-up, irrevocable, world-wide license to publish or reproduce the published form of this article or allow others to do so, for United States Government purposes. The DOE will provide public access to these results of federally sponsored research in accordance with the DOE Public Access Plan https://www.energy.gov/downloads/doe-public-access-plan.

Kristin B. Zimmerman, PhD (eds.), *Special Topics & Experimental Techniques in Structural Dynamics, 2026, Vol. 5*, Conference Proceedings of the Society for Experimental Mechanics Series, https://doi.org/10.1007/978-8-743-81444-3_3

interest in replacing these with multi-axis tests [3, 4]. Cross et al. recently proposed a new and robust multi-shaker system which they named the Natural Excitation Within a Test frame (NEWT) [5]. The NEWT frame is built using standard 3x3 in. (76x76 mm) 80/20 beams (i.e. see http:\8020.net) and designed with a high degree of modularity, so one can use it to position a large number of shakers around a test article and reproduce the article's dynamic response in all axes simultaneously and up to levels comparable to those achieved on large shaker systems [5]. A NEWT frame is relatively inexpensive (i.e. compared to commercial, multi-axis test systems) and, because it is modular, it is easy to replace a shaker that becomes damaged in the course of testing.

Although the NEWT frame has been shown to be capable of replicating realistic dynamic environments, vibrations within the NEWT frame itself seem to limit the performance of the system. It has been observed that the shakers sometimes draw increasing amounts of electrical power and yet are still unable to reach the desired test conditions. The problem can sometimes be remedied by rearranging the shakers or tightening connections to the frame, or other adjustments. While the authors are not aware of a work that has studied this in detail, these problems are thought to occur due to antiresonances between particular shakers and the control accelerometer(s). An antiresonance in one of the shaker-control accelerometer transfer functions would cause the voltage to the shaker to increase significantly over a narrow range of frequencies. The aim of this study is to recreate a NEWT test frame, document a simplified baseline vibration environment in a Single Input Single Output (SISO) test, and develop passive vibration mitigation solutions for the recreated frame that reduce 1.) the vibration in the frame and 2.) the power input to the shakers when achieving a basic vibration environment in a component. This solution can then be applied in the future to a multi-shaker, Multiple Input Multiple Output (MIMO) testing frame, such as that in [5].

The effect of vibration within a similar frame was recently studied by Kramer et al. [6], who constructed a two-shaker frame and evaluated its performance in two configurations: with viscoelastic strips added to increase its damping, and with bars and cross braces added to increase its stiffness. They showed that both treatments changed the mode shapes of the frame, although any increase in damping was not quantified, nor was the change in stiffness. On the other hand, they found that all frames had control difficulty leading to over-test (i.e. resonances where the shaker voltage could not be made low enough to avoid exceeding the acceleration environment) at exactly the same frequencies. They also showed that all frames had nearly the same inverse FRFs, i.e. voltage over acceleration, indicating that the treatments did not alter the anti-resonances significantly. This is peculiar, because vibration absorber (or tuned-mass damper) theory [7] shows that the depth of an antiresonance decreases as damping is increased.

This study builds on [6] in several ways. First, the frame studied here is constructed from stiffer 3 in. (76 mm) 80/20 tubes, so it is similar to that of Cross et al. [5]. Specifically, a NEWT frame was constructed from 14 extruded 80/20 aluminum bars, sized 3x3x30 in (76.2x76.2x762 mm) and 3x3x36 in (76.2x76.2x914 mm), total dimensions of 36x36x36 in (914x914x914 mm), as shown in Figure 4a, and is the subject of this study. Second, we quantify the effect of two different damping treatments on the frame. Particle damping, the use of freely moving particles confined in a cavity, has been studied as a passive damping solution [8, 9, 10], and is implemented here. A roving hammer modal test is used to quantify the effect of the particle damping treatment on a single beam in the test frame, and on the frame as a whole, and found to increase the damping by an order of magnitude or more at some frequencies. Another common damping solution is to add viscoelastic material between components, typically in a way that minimizes the transmission of vibrations from one part to another. In our study this is done by inserting viscoelastic pads between the beams comprising the frame or beneath the shaker.

For both damping treatments, we construct a closed-loop control problem in which antiresonances are present and quantify the reduction in the shaker drive voltage required to reach the environment of interest on the Device Under Test's (DUT). In these tests, the vibration in the test frame was measured with an accelerometer recording along the axis of the shaker. The voltage and current to the shaker were also measured to quantify the effect of antiresonances on the voltage required to reach the environment.

Note that, while this study focuses solely on passive damping solutions, other ideas were considered. We also considered implementing a tuned mass damper. A tuned mass damper is passive, but is typically tuned to address a resonance at a specific frequency, such as the natural frequency of a building [11]. We attempted to implement two such techniques, but found that it was difficult to tune them for the anti-resonance frequencies of interest. Indeed, considerable experimentation was required to even identify the anti-resonances that contributed most to difficulties in our test system. Additionally, all of the tuned mass damper designs that we attempted were found to add several other modes to the system, potential creating new antiresonances and exacerbating the problem rather than addressing it. Hence, in the end we decided to focus on solutions that increased the damping in the frame over a wide (20-2000 Hz) range of frequencies.

The following section details the damping methods used and the tests that were performed. Results of those tests are presented in Sec. , followed by conclusions in Sec. .

Methods

To evaluate the performance of damping methods on a simple system, we initially performed roving hammer modal testing on a single, suspended 80/20 beam. We tested the beam both with and without the central cavity filled with silica, in order to document the baseline effectiveness of particle damping on the dynamics of the beam (Figure 1). Roving hammer testing was then performed on a completed NEWT frame with and without particle based damping treatments applied to compare the effect of the damping on the modes existing within a complex test frame. Another test we used to quantify the damping effect on the frame was a random noise vibration test on a DUT with both a damped and undamped test frame.

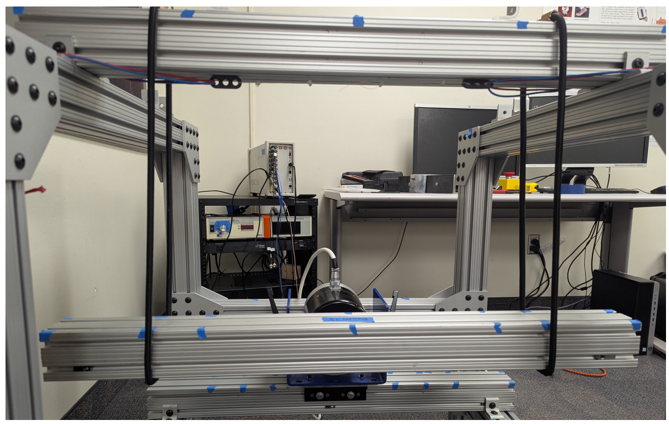

Fig. 1 Picture of experimental setup for roving hammer tests

Single Beam Roving Hammer Testing

A 3x3x36 in. (76.2x76.2x914.4 mm) 80/20 beam was suspended, without particle damping treatment, by bungee cables to approximate free-free boundary conditions and isolate the beam modes from any existing modes of the frame. A modal hammer test was used to measure Frequency Response Functions (FRFs) of the beam at 10 points along the top and side faces of the beam as shown in Figure 2. Each point was struck in the x and z directions, with corners also being struck in the y direction, to obtain 24 FRFs.

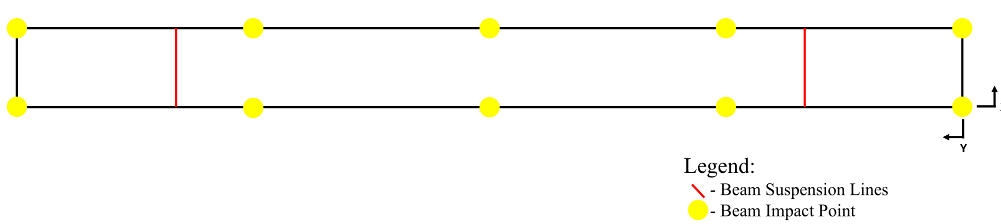

Fig. 2 Top view sketch of hammer impact points

The natural frequencies, damping ratios and mode shapes of the beam were obtained from the measured FRFs using the Algorithm of Mode Isolation (AMI) [12]. By isolating the modes of the beam and fitting modal model to the FRF, damping ratios were calculated for each configuration. To test the damped system, the hollow core of the beam was filled with approximately 1.7 L of 4075 white silica sand and end caps were placed at the end of each beam, as shown in Figure 3, to prevent leakage. This volume of sand fills the beam fully without packing. The modal hammer test was repeated using the same parameters and a new FRF of the damped case was produced.

Full Frame Roving Hammer Testing

To examine how the damping affected modal behavior within a complex frame, a modal hammer test using the same testing hardware as the single beam test was performed, with impact points being selected at the corners and midpoints of select

Fig. 3 Picture of beam with plastic end cap, One cap was used on each end and the cavity was filled with silica

beams to simplify the analysis as shown by the small squares in Figure 4b. This test was performed first on an undamped frame and then on the same frame with all the beam cores filled with approximately 1.7 L (1.4 L in the shorter 30 in beams) of white silica sand and sealed with end caps to prevent leaking. For both tests, FRFs were generated and damping ratios calculated for each identified mode using the same methods as in the single beam tests.

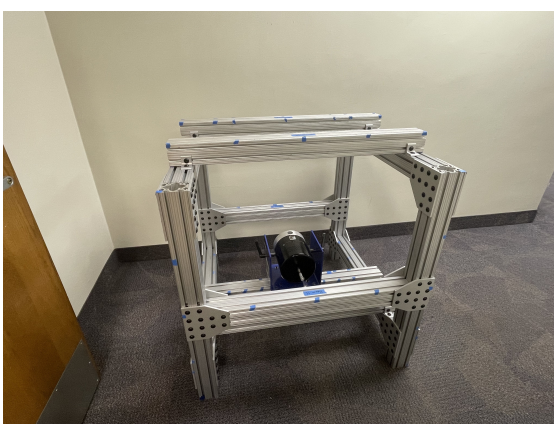

(a) Completed NEWT frame

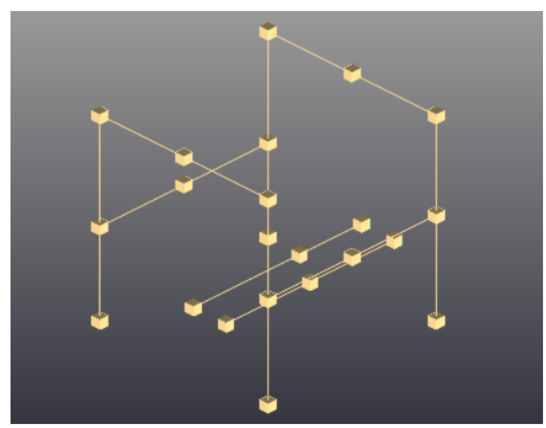

(b) Test Geometry in Siemens TestLab®

Fig. 4 Experimental setup for hammer tests of the complete frame

Random Noise Vibration Testing

Using the same test frame from our full-frame roving hammer tests, we bolted a single Modal Shop Shaker Model 2075E to a crossbeam and oriented it parallel to the ground. The shaker was connected to an acrylic stinger with an aluminum collar as shown in Figure 5. The stinger was then fastened to a second aluminum collar which was attached to the DUT using super glue. We attached a control accelerometer opposite the stinger connection point on the DUT. To monitor frame behavior during the test, we also attached a second accelerometer to the test frame along the axis of actuation on the bem on which the shaker was mounted. To monitor the power going to the shaker, we recorded the voltage output of our control system in the software and recorded the current using a current probe attached to the shaker power cable.

For our controller we used a DataPhysics Abacus and the Random Noise package from the SignalStar Matrix software. The Data Physics system automatically computes the drive voltage needed by the shaker to match a given environment at the control accelerometer over the frequency range of interest (20-2000 Hz). The software measures and stores the Power Spectral Density (PSD) and FRF of the control accelerometer, of the accelerometer on the base of the frame, and of the voltage sent to the shaker. Current PSDs were also recorded in some tests, and found to have a similar appearance to the voltage PSDs, so this paper focuses on the voltages.

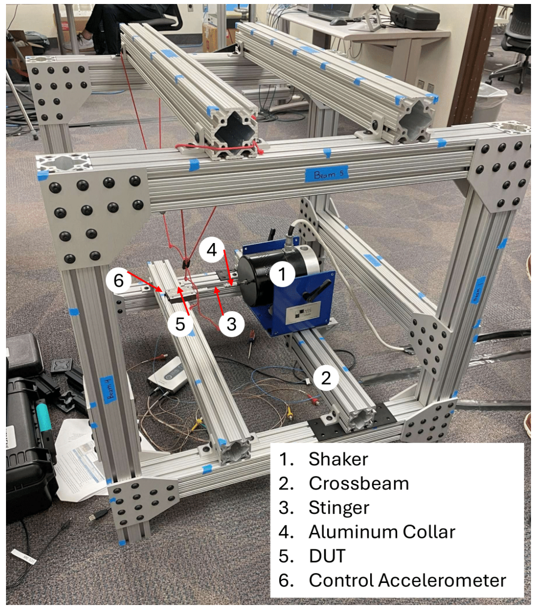

Fig. 5 Labeled image of the initial test configuration for random vibration testing

During initial tests, we used both a 1 lb mass and a 10 lb dumbbell as DUTs. We hung the DUT from Kevlar thread, which we then suspended from a crossbeam using bungee cables to approximate free-free boundary conditions and minimize energy being transmitted through the DUT into the test frame. With this test setup, no antiresonances were identified by visual inspection of PSDs or FRFs generated by the SignalStar software (see Appendix A, Figure 18). We hypothesize that it may not be possible to obtain anti-resonances in a single-shaker system with a rigid DUT, as the dynamic coupling of multiple shakers through the DUT and frame cause the undesirable antiresonances. As only one shaker was available, we simulated this multi-shaker coupling by using the single shaker to drive one of the cross beams of the frame. We established a direct connection to a horizontal cross beam of the frame using dental cement between the DUT beam and the stinger collar (Figure 6). The dental cement replaced Loctite super glue because the super glue failed and caused separation from the beam during testing. With the new setup, we were able to visually identify several frequencies at which antiresonance occured, as shown in Figure 11, which is described subsequently.

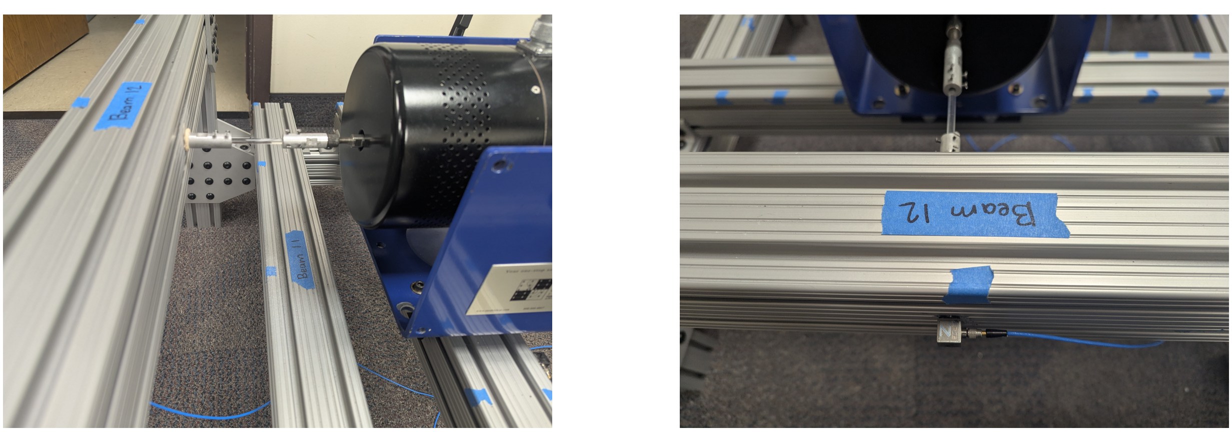

(a) Shaker connection to DUT crossbeam (b) Control accelerometer and shaker

Fig. 6 Photos of the Random Noise experimental setup

Using this configuration, we ran random noise tests with a maximum voltage output of 3 V to the amplifier to prevent damage to the shaker, a reference acceleration of $5 \times 10^{-8} g^2$/Hz, and a frequency range of 20-2000 Hz. These tests were repeated across several undamped cases before adding particle damping or viscoelastic isolation. For the particle damped

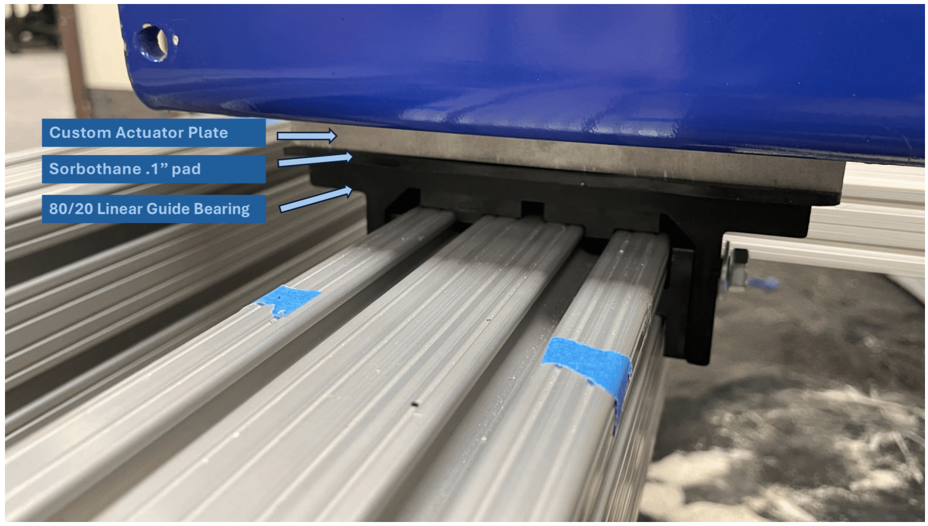

Fig. 7 Image of viscoelastic isolator installation with labels

tests, all beams comprising the frame were filled as previously mentioned. For viscoelastic isolation, 70 duro Sorbothane, 0.1 in (2.54mm) thick pads were placed between the shaker and the test frame as shown in Figure 7.

Results

Roving Hammer Tests

Each peak in the FRF plots is a resonance within the test frame. Figure 8 shows the composite (or average) of the measured frequency responses from both the single-beam and full-frame tests. In both cases the system with silica sand (plotted as a red line) has wider, less sharp resonances, indicating an increase in damping. The single beam shows only about five major resonances, so this effect is clear for that system. In contrast, for the undamped frame at least 136 resonances were identified below 2kHz, while only about 25 could be extracted once the silica was added to the frame. Additionally, the silica is seen to be most effective above about 300 Hz; modes below that frequency do not show a strong increase in damping.

The damping ratios for both systems were estimated from the measured FRFs using AMI, and are shown in Figure 9. The 80/20 beam without any treatment had damping ratios around 0.001, and these increased to 0.01-0.1 when the beam was

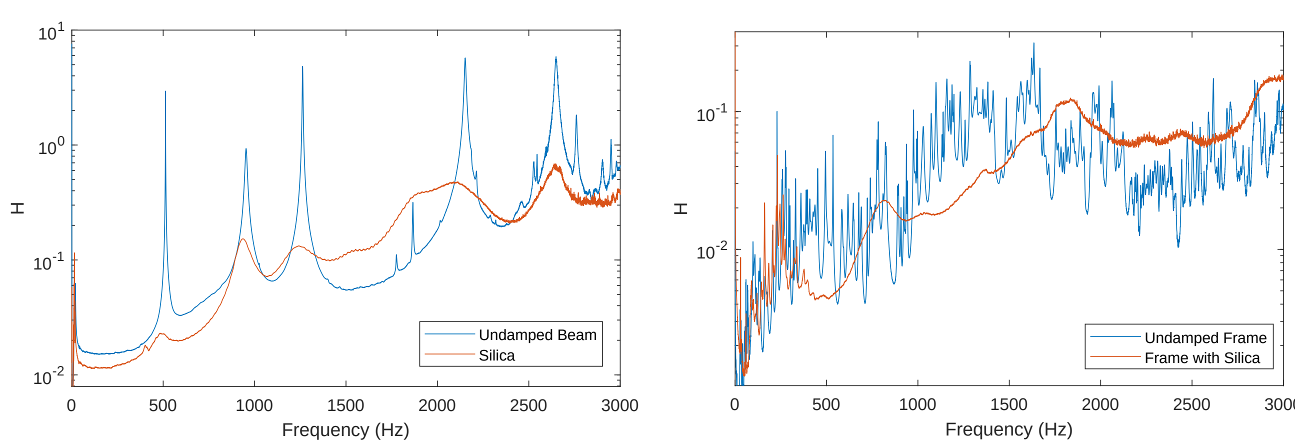

(a) Single Beam Composite of (24x1) FRF Matrix (b) Full Frame Composite of (36×3) FRF Matrix

Fig. 8 Composite frequency responses from roving hammer tests. Red lines show the result for the system damped using silica powder and blue lines show the undamped system filled with silica, an increase by a factor of 10-100. The damping in the full frame in the undamped configuration was a bit higher, between 0.001-0.005 for the higher frequency modes, and as high as 0.03 for the lower modes, as seen in Figure 9b. This increase in damping is presumed to come from the bolted joints in the assembly. The silica increases the damping of the higher frequency modes to about 0.05-0.08, an increase of a factor of 10-80. Granted, the damping was large enough in the high frequency modes that it was hard to extract reliably. In contrast, the damping ratios of the modes below about 300 Hz are similar to those of the bare frame. The silica seems to add relatively little damping at those frequencies. Those frequencies are below the first bending mode of a free-free 80/20 beam.

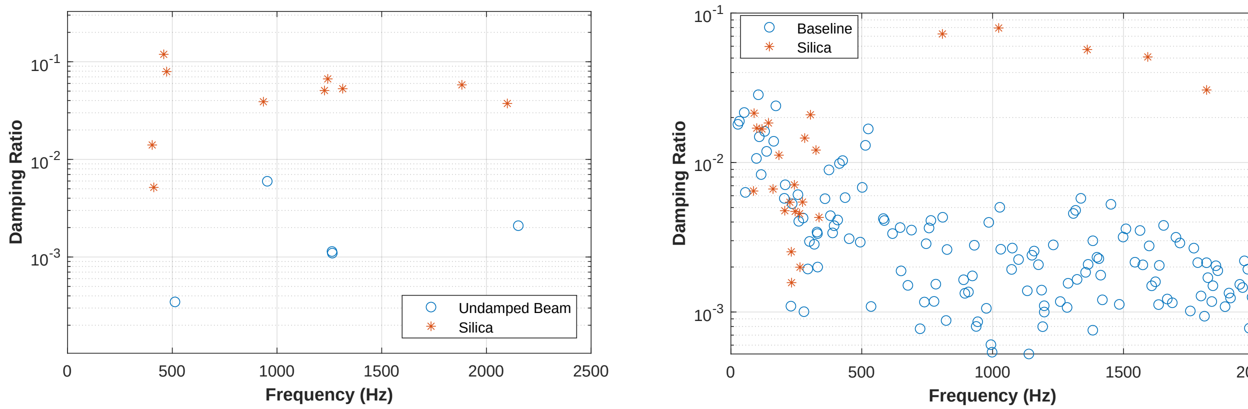

(a) Damping Ratios of Single Beam (b) Damping Ratios of Full Frame

Fig. 9 Damping ratios extracted from roving hammer test on each system

The mode shapes of the full frame were examined to confirm the type of motion that was present at each frequency. A few sample mode shapes are shown in Figure 10. The modes below 100 Hz seemed to be dominated by the stiffness of the joints, with the beams moving rigidly. At about 100 Hz the vertical (Z-direction) beams begin to show first-mode type deformation (e.g. see Mode 5 in Figure 10b), and by 500 Hz the cross beams can be seen to bend as well (see Mode 41 in Figure 10c). Higher modes are expected to correlate to higher order bending of the various beams that comprise the frame, although the measurement grid used wasn't sufficient to visualize those modes.

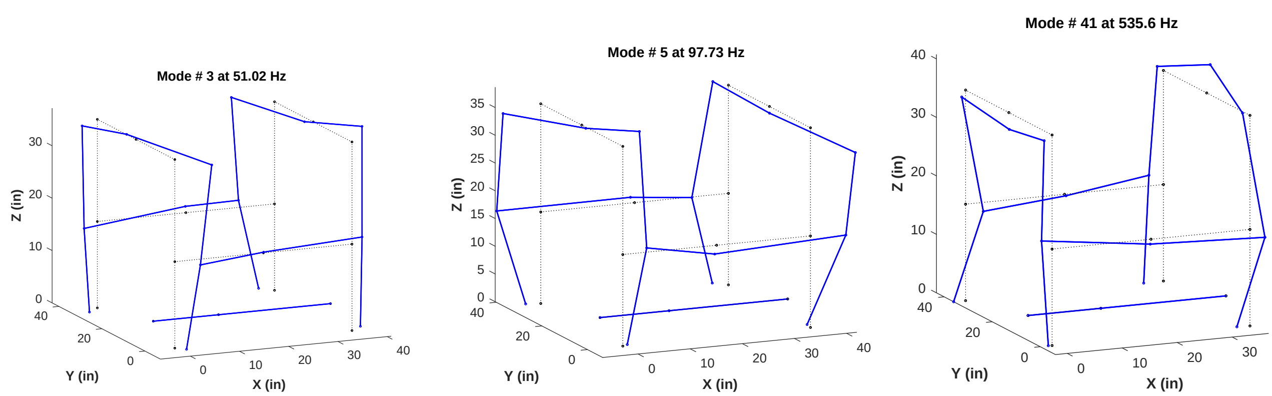

(a) Mode 3 at 51.0 Hz (b) Mode 5 at 97.7 Hz (c) Mode 41 at 535.6 Hz

Fig. 10 Deformation Shapes of Selected Modes. Dashed black lines show the undeformed frame, while blue lines show the deformation pattern of the mode in question

Random Vibration

Frequency Response Function and Power Spectral Density

One of the most useful sets of data from the random vibration shaker tests is the FRF, a ratio of DUT acceleration to the shaker voltage input. This information shows how much voltage is needed to simulate a test environment of a certain amplitude and frequency. These plots show at what frequencies resonances and antiresonances occur as indicated by peaks and valleys respectively. At antiresonances, the shaker requires a large amount of voltage to achieve a given amplitude of vibration in the DUT, which potentially compromises controllability of the DUT. Significant antiresonances were visually identified at around 580, 616.25, and 1357.5 Hz from Figure 11. The severity of the antiresonance and its effect on controllability can be gauged by the depth of the valley in the acceleration FRF.

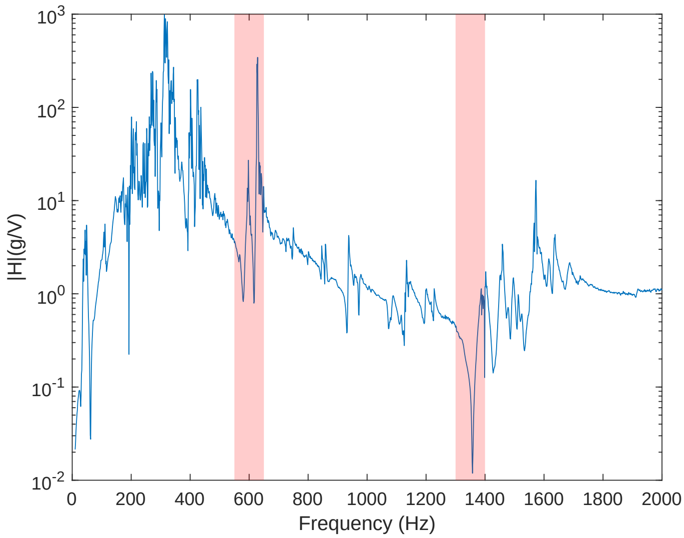

Fig. 11 Control accelerometer FRF with the undamped frame. Antiresonance bands used for the RMS values are highlighted in red

Each antiresonance indicates a frequency in which the vibration at the control accelerometer is minimal for a given shaker voltage. Per the well known theory [7], the energy from the shaker is driving vibration in other parts of the structure, which vibrate in a way that cancels the applied force, allowing the control accelerometer to remain stationary. Antiresonances generally emerge due to a linear combination of the modes near the antiresonance frequency. To obtain an understanding of how the frame might move in each antiresonance, some of the modes that were identified from the data in Figure 8b are shown in Figure 12. The control accelerometer is located near the center of the beam in the front of the frame (near $(x, y, z) = (16, 0, 15)$ in those figures). For the first two antiresonances, it seems that the lateral bars (along the x-axis) vibrate, as do the top corners of the frame, to cancel the motion at the control accelerometer. The antiresonance at 1357.5 Hz, which is the strongest in Figure 11, seems to involve motion of the top of the frame and motion of the legs where they rest on the carpet.

Another important data set from the random vibration shaker tests is the PSD of the voltage sent to the shaker. Because the DUT is controlled to a constant amplitude across the frequency range, the voltage PSD looks very similar to the reciprocal

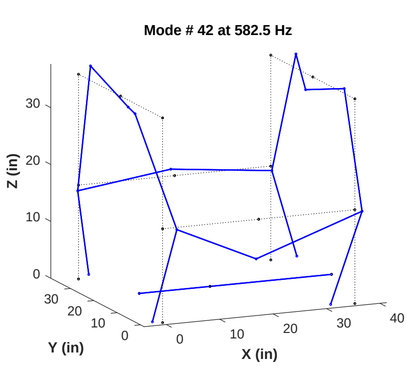

(a) Mode 42 at 582.5 Hz

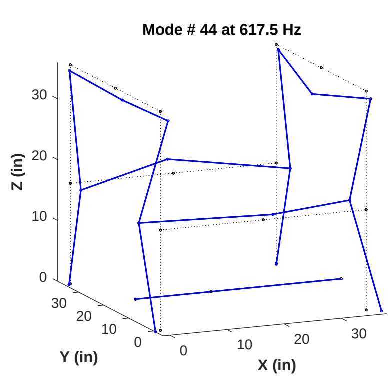

(b) Mode 44 at 617.5 Hz

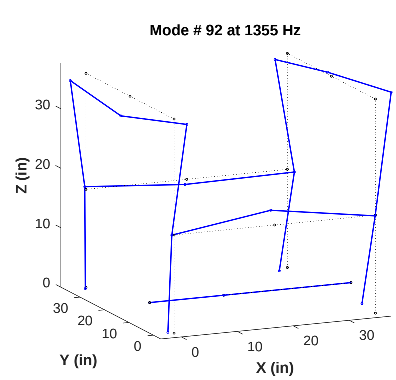

(c) Mode 92 at 1355 Hz

Fig. 12 Deformation shapes of the modes identified from the data in Figure 8b nearest to each antiresonance in Figure 11 of the acceleration FRF. This means that antiresonance points are characterized by peaks instead of valleys. The PSD can be integrated over a frequency band to find a Root Mean Squared value (RMS) of the voltage over that range of frequency. In our analysis, we compared the RMS voltages from a broadband range of 20-2000 Hz as well as narrower bands at 550-650 Hz and 1300-1400 Hz. These two narrower bands focus on identified antiresonances.

Undamped System Sensitivity

While performing the random vibration shaker tests on the undamped frame, is was noted that the dynamics of the frame and DUT are very sensitive to setup and are challenging to recreate. For example, the torque to which the frame bolts are tightened significantly alters the system dynamics. Figure 13 shows the results from an undamped shaker test with the frame joints tightened to 11 ft-lb as well as an undamped test with 8 ft-lb bolted joints. The change in bolt torque caused both a frequency shift and amplitude changes to minima and maxima in the plots. The resonance and antiresonance frequencies typically shifted upwards as the bolt torque increased, which makes sense considering that higher torques likely increase the stiffness of the joints. The difference in amplitude of the antiresonances is quantified by the RMS values of those frequency bands, which are shown in Table 1.

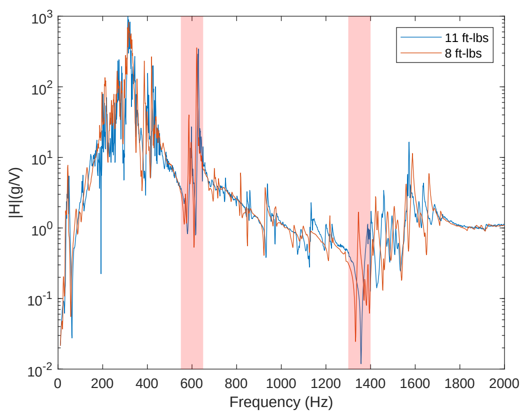

(a) Control accelerometer FRF

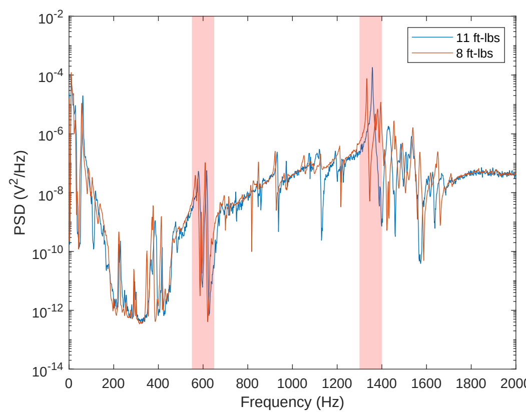

(b) Shaker voltage PSD

Fig. 13 Comparison of random noise results when using an undamped frame with variable bolt torque at joints

Table 1 Comparison of voltage RMS values for an undamped frame at different frame bolt torques

	Voltage RMS Over Antiresonance Bands (V^2)		
	550-650 Hz	1300-1400 Hz	20-2000 Hz
11 ft-lb	$7.556 * 10^{-7}$	$8.583 * 10^{-4}$	$1.097 * 10^{-3}$
8 ft-lb	$8.415 * 10^{-8}$	$4.437 * 10^{-4}$	$6.369 * 10^{-4}$

Even while holding bolt torque in the frame constant, removing beams from the frame and then reattaching them in the same location significantly changed the amplitude of resonances and antiresonances. Figure 14 shows FRFs and PSDs of multiple undamped tests. Between each of these runs, the frame was partially disassembled and then reassembled with identical geometry and bolt tightness. While the general profile of these plots remains constant, there are differences in the amplitudes of the minima and maxima. This is an especially important result for large valleys in the FRF where frame antiresonances occur as these require significant increases in the shaker voltage and hence could make the test impossible to run using the given shaker.

Viscoelastic Isolators

As discussed above, the antiresonances were found to move when the system was disassembled and reassembled. As a result, we had difficulties justifying which undamped test the viscoelastic material was comparable to since we had to loosen bolt torques and change other boundary conditions in order to add it to the frame. We repeated viscoelastic and undamped tests

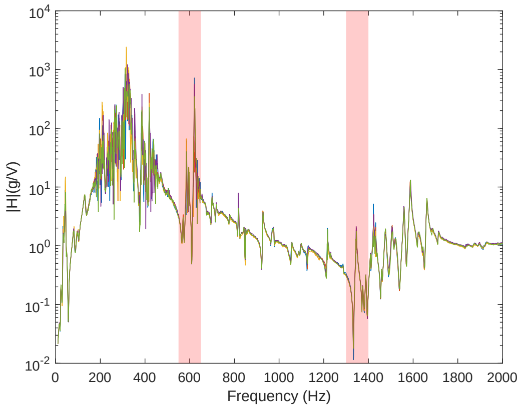

(a) Control accelerometer FRF

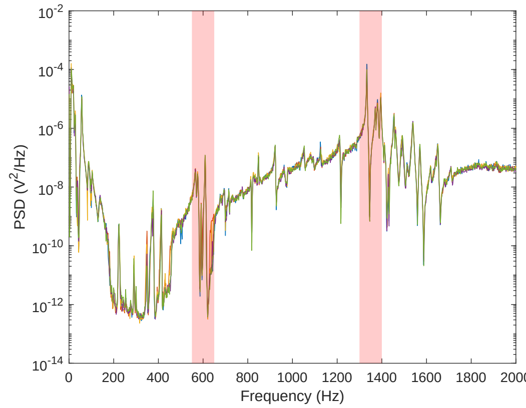

(b) Shaker voltage PSD

Fig. 14 Comparison of results across several random noise tests with no change to frame parameters

in an attempt to get a better idea of what the factor of improvement would be. During this testing, we also tested a few configurations of the viscoelastic material to determine which was the most effective. The viscoelastic material was tested in two places: 1.) between the shaker and linear slider and 2.) between the shaker beam and the rest of the frame. Additionally, several different bolt torques were used on the bolts attaching the viscoelastic to the frame. Two rounds of testing with viscoelastic are shown below. In the first, the bolts for the frame were tightened to 11 ft-lb everywhere except where the viscoelastic was placed. The bolts used to tighten the viscoelastic were only tightened to 8 ft-lb, as this seemed to give the largest improvement.

As shown in Figure 15, there were two major bands where antiresonance problems were found. Looking at the FRF, the antiresonances occurred at 580, 616.25, and 1357.5 Hz. By visual inspection of the FRF, we can see that the viscoelastic material helped the antiresonances by reducing the depth of the valley in the graph. This can quantified by finding the RMS value from the PSD, as shown in the three rightmost columns in Table 2. Three RMS values were obtained from each of the PSDs in Figure 15b. The RMS value for the 550-650 Hz band gives the average change over the first two antiresonances, while the 1300-1400 Hz band focuses on the antiresonance at 1357.5 Hz. Additionally, the RMS value is given for the entire frequency range (20-2000 Hz) as the last column in Table 2. The viscoelastic material reduced the RMS voltage at both antiresonances, although the factor of improvement was larger for the higher frequency antiresonance. It can also be seen in Figure 15a that the viscoelastic treatment shifts and damps several modes of the system in the 100-500 Hz region, and seems to generally increase the damping. This frequency band does not produce significant antiresonances in this setup, so this doesn't affect the RMS shaker voltage required. Nevertheless, this does suggest that the sorbothane is improving the dynamics of the system.

Table 2 Comparison of voltage RMS values for a frame with and without Sorbothane padding with frame bolts tightened to 8 and 11 ft-lb

Voltage RMS Over Antiresonance Bands (V^2)						
	8 ft-lb (see Figure 15)			11 ft-lb (see Figure 16)		
	550-650 Hz	1300-1400 Hz	20-2000 Hz	550-650 Hz	1300-1400 Hz	20-2000 Hz
No Treatment	$8.415 * 10^{-7}$	$4.437 * 10^{-4}$	$6.368 * 10^{-4}$	$7.556 * 10^{-7}$	$8.583 * 10^{-4}$	$1.097 * 10^{-3}$
Sorbothane	$6.730 * 10^{-7}$	$2.018 * 10^{-4}$	$5.094 * 10^{-4}$	$4.393 * 10^{-7}$	$1.571 * 10^{-4}$	$3.834 * 10^{-4}$
Improvement	1.252	2.199	1.250	1.720	5.463	2.861

Another set of tests was performed and the results are shown in Figure 16. For these tests, the frame was disassembled and reassembled with all of the bolt torques at 8ft-lb.

This second sets of results demonstrates a problem encountered with viscoelastic material. Though the viscoelastic material still helped at the antiresonance problem bands, the factor of improvement was less than previous tests. The numerical results are shown in the left three columns in table 2. With the lower preload on the bolts, Figure 16a shows that the 650-1300 Hz frequency band has a similar character to that observed in Figure 15a, however, this FRF has a new antiresonance

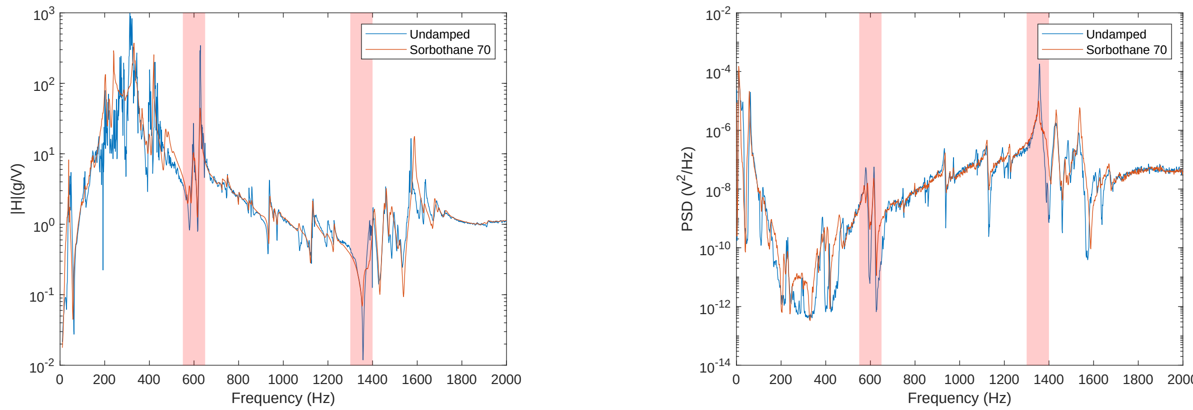

(a) FRF (b) Shaker voltage PSD

Fig. 15 Comparison of results across random noise tests with and without Sorbothane pad with 11 ft-lb preload on the frame bolts

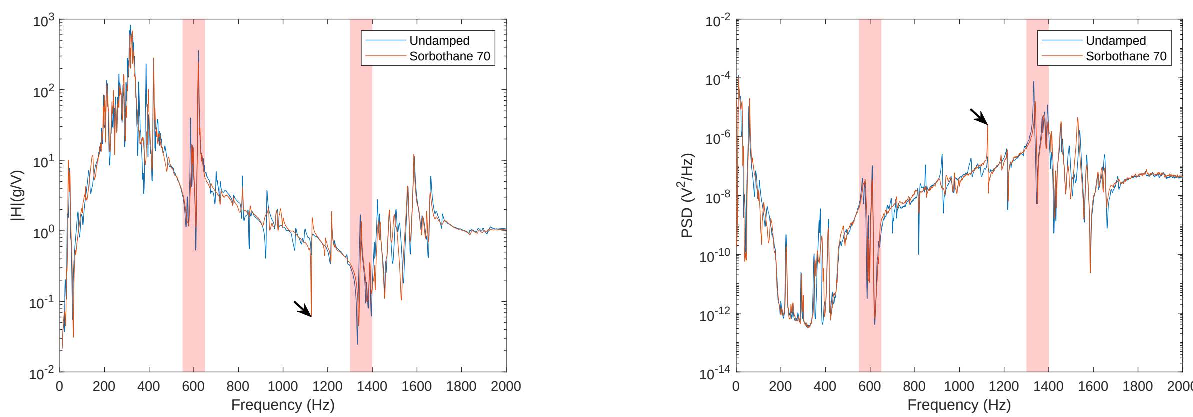

(a) FRF (b) Shaker voltage PSD

Fig. 16 Comparison of results across secondary random noise tests with and without Sorbothane pad with 8 ft-lb preload on the frame bolts

at 1126.3 Hz, which would increase the shaker voltage at this frequency and likely causes issues for controllability. Visually, the modes around 100-500 Hz in Figure 16a were not damped as much as seen in Figure 15a. Additionally, Sorbothane moved many of the resonances and antiresonances making the tests less predictable and harder to compare. We were unable to conclude why this antiresonance appeared in this test and not in the others; further research would be needed to understand why this antiresonance appeared.

Silica Particle Damping

Some of the most interesting and promising results came from testing the silica particle damping-treatment. Figure 17a shows that silica adds significant damping to the FRF between the control accelerometer and the shaker voltage. Many of the extrema are completely smoothed, especially above 700 Hz. Hence, the voltage PSD in Figure 17b is also smoother. Visually, the shaker voltage doesn't have significant peaks at any of the identified antiresonances. Quantitatively, this is reflected in the RMS values over the bands of interest as shown in Table 3. Around the lower antiresonance, the silica decreased the voltage RMS by a factor of 8.67. At the higher antiresonance, the factor of improvement is 20.51. Note that the voltage RMS over the whole frequency range improves by only a factor of 2.65. This is because the RMS shaker voltage over the entire frequency band is dominated by a peak at 60 Hz. If the RMS was instead computed over the 100-2000 Hz band, the RMS voltage decreased by a factor of 4.8 instead of 2.65.

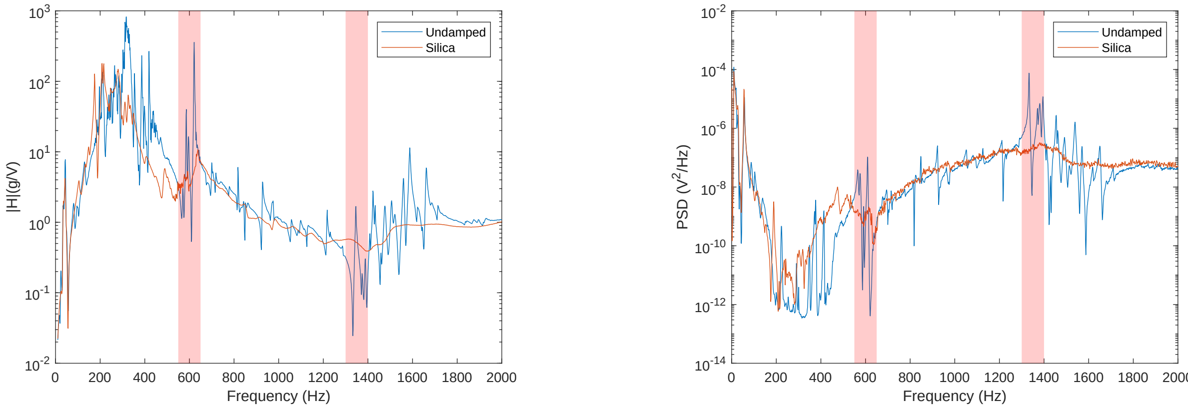

(a) Control accelerometer FRF (b) Shaker voltage PSD

Fig. 17 Comparison of results across random noise tests with and without silica particle damping

Table 3 Comparison of voltage RMS values for a frame with and without silica particle damping

Voltage RMS Over Antiresonance Bands (V^2)			
	550-650 Hz	1300-1400 Hz	20-2000 Hz
No Treatment	$8.415 * 10^{-7}$	$4.437 * 10^{-4}$	$6.368 * 10^{-4}$
Silica	$9.711 * 10^{-8}$	$2.1632 * 10^{-5}$	$2.399 * 10^{-4}$
Improvement	8.67	20.51	2.65

While this treatment performs well for the antiresonances that are of primary interest, and in general at mid to high frequencies, there remain significant dynamics below 700 Hz. The same was seen in our roving hammer test results (e.g. see Figure 8b) where it was noted that particle damping was less effective below 500 Hz. If a test setup has antiresonances below 500 Hz, one would imagine that it is typically possible to reconfigure the frame to move them up to higher frequencies. Hence, these results suggest that silica particle damping can be an effective damping treatment to counter test frame antiresonances.

Conclusions

This study explored passive damping solutions to mitigate vibration in a frame similar to the NEWT frame [5], which was recently proposed by Sandia National Laboratories to facilitate multi-shaker testing. It was found that using particle damping in the frame, by filling the hollow center of the beam with silica sand, significantly increased the damping in the frame, particularly above 500 Hz. This lowered the amplification of most of the frame's resonances and decreased the power draw of the shaker at the antiresonances. The silica damping treatment is ready to undergo testing in a full-scale MIMO frame with many shakers.

This study also explored other damping treatments. In particular, viscoelastic (Sorbothane) pads placed at the interface between the shaker and frame had varying degrees of success, depending on the configuration. They were generally found to increase the damping in the system, but they also moved resonances and anti-resonances, sometimes increasing the voltage needed by the shaker.

The antiresonances that were found in this study were not easy to predict, and they were found to change noticeably if the system was disassembled and reassembled. Hence, future studies should pay close attention to the configuration; damping is only expected to reduce the shaker voltage requirements when it reduces the severity of an antiresonance. While not elaborated here, several other configurations were studied as part of this work, and the acceleration to voltage FRF for one of these is shown in Figure 18; it does not exhibit any antiresonances and hence the damping treatment didn't change the shaker voltage for that setup.

References

1. Rudder, F. and Plumblee, H.E. "Sonic Fatigue Design Guide for Military Aircraft". Technical report, Flight Dynamics Laboratory, Wright-Patterson AFB, Ohio (1974)ifnextchar.gobble.
2. Foley, J. "Normal and abnormal dynamic environments encountered in truck transportation". *The Shock and Vibration Bulletin*, 39:31 (1969)ifnextchar.gobble.
3. Daborn, P.M., Roberts, C., Ewins, D.J., and Ind, P.R. "Next-Generation Random Vibration Tests". In Allemang, R., editor, *Topics in Modal Analysis II, Volume 8*, Conference Proceedings of the Society for Experimental Mechanics Series, pages 397–410, Cham (2014)ifnextchar.gobble. Springer International Publishing.
4. Schoenherr, T.F. "Derivation of Six Degree of Freedom Shaker Inputs Using Sub-structuring Techniques". In Mains, M. and Dilworth, B.J., editors, *Topics in Modal Analysis & Testing, Volume 9*, pages 5–14. Springer International Publishing, Cham (2019)ifnextchar.gobble. Series Title: Conference Proceedings of the Society for Experimental Mechanics Series.
5. Cross, K., Melendez, G., and Zwink, B. "Natural excitation within a test-frame: Experimental results". Proceedings of IMAC - International Modal Analysis Conference. IMAC (2023)ifnextchar.gobble.
6. Kramer, H., Schultze, J., Danforth, S., and Mann, B. "Dynamic analysis of a modular test stand for multi-axis vibration testing". Proceedings of IMAC - International Modal Analysis Conference. Unpublished Manuscript (2025)ifnextchar.gobble.
7. Ginsberg, J.H. *Mechanical and Structural Vibrations: Theory and Applications*. John Wiley and Sons, New York, 1st edition (2001)ifnextchar.gobble.
8. Lu, Z., Wang, Z., Masri, S.F., and Lu, X. "Particle impact dampers: Past, present, and future". *Structural Control and Health Monitoring*, 25 (2017)ifnextchar.gobble.
9. Lu, Z., Wang, Z., Masri, S.F., and Lu, X. "Particle impact dampers: Past, present, and future". *Structural Control and Health Monitoring*, 25(1):e2058 (2018)ifnextchar.gobble. _eprint: https://onlinelibrary.wiley.com/doi/pdf/10.1002/stc.2058.
10. Hollkamp, J.J. and Gordon, R.W. "Experiments with particle damping". volume 3327 of *Proceedings of SPIE - The International Society for Optical Engineering*, pages 2–12. SPIE (1998)ifnextchar.gobble.
11. Zhou, K. and Li, Q.S. "Vibration mitigation performance of active tuned mass damper in a super high-rise building during multiple tropical storms". *Engineering Structures*, 269 (2022)ifnextchar.gobble.
12. Allen, M.S. and Ginsberg, J.H. "A Global, Single-Input-Multi-Output (SIMO) Implementation of The Algorithm of Mode Isolation and Applications to Analytical and Experimental Data". *Mechanical Systems and Signal Processing*, 20:1090–1111 (2006)ifnextchar.gobble.

Appendix A

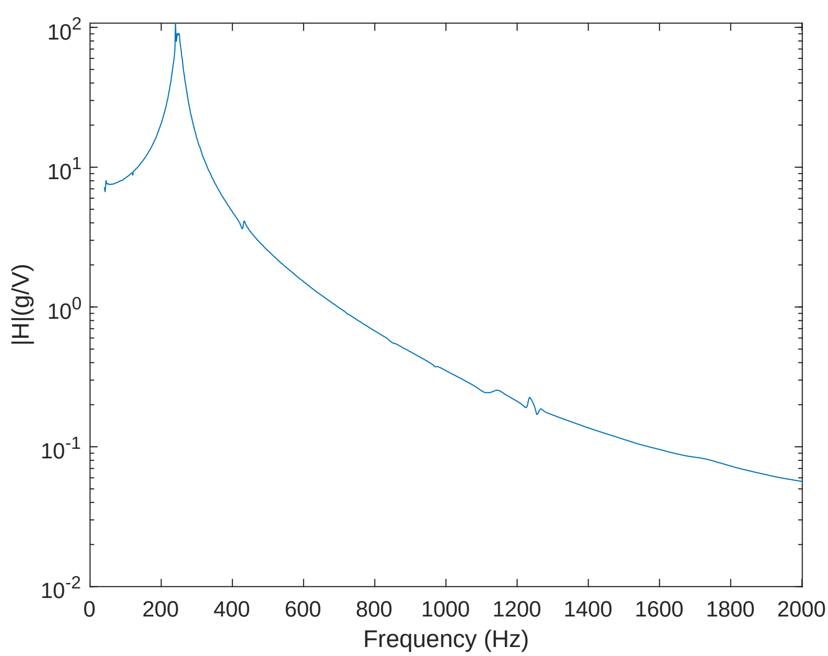

Fig. 18 Undamped FRF between DUT acceleration and shaker voltage, with 10 lb mass used as the DUT, demonstrating the lack of antiresonances